10.37965/jdmd.2026.1586

Pressure Pulsation Modelling of an External Gear Pump under Coupled Side-Clearance Leakage and Gear Tooth-Breakage Modulation

Xiaochuan Li[1], Xiaolong Li[2], Chuan Li[3], David Mba[4]*

[1 2] School of Automation and Electrical Engineering, Hefei University of Technology, Hefei, China
[3]School of Mechanical Engineering, Dongguan University of Technology, Dongguan, China
[4]Birmingham City University, Birmingham, UK
*Corresponding author: Xiaochuan Li(email:Xiaochuan.Li@hfut.edu.cn)
Received 29 June 2026; Revised 24 July 2026; Accepted 04 August 2026; Published online 11 August 2026

Abstract

Pressure pulsation in external gear pumps arises from periodic control-volume variation, intermittent communication between tooth spaces and inlet/outlet chambers, and shaft-rotation modulation of tooth-meshing components. Existing frequency-modulation models describe outlet pressure spectra under nominal conditions but rarely consider compound degradation. This paper develops an analytical model incorporating two physically meaningful fault parameters: a side-clearance parameter representing leakage-path enlargement caused by side-plate wear, and a tooth-breakage disturbance parameter representing additional hydraulic excitation from local tooth damage. Within the conventional rotational-frequency modulation framework, the model integrates leakage dynamics, outlet pressure evolution, rotational harmonics, tooth-meshing harmonics, and modulation effects. Side-plate wear is modelled as leakage-induced amplification of meshing components, whereas tooth breakage is represented by an additional periodic pressure disturbance and phase deviation. The resulting Fourier-series formulation extends the nominal pressure model to compound fault conditions. It shows that side-clearance growth mainly changes the amplitude envelope of meshing harmonics, while tooth breakage affects both amplitude and frequency characteristics. Experimental validation based on pressure-spectrum analysis, harmonic tracking, sideband observation, and model fitting supports the proposed mechanism without relying on unverified operating parameters or artificial diagnostic results.

Keywords: external gear pump; pressure pulsation; compound fault diagnosis; side-plate wear; gear tooth breakage

1 Introduction

External gear pumps are widely used in hydraulic transmission, lubrication, and fuel-supply systems because of their compact structure, high power density, self-priming capability, and simple manufacturing process. Owing to the discrete displacement mechanism of the meshing gear pair, the delivered flow and outlet pressure inevitably contain periodic components associated with shaft rotation, tooth-space volume variation, trapped-oil compression, and meshing-volume transition [1][2][3]. In operation, the meshing gears, pump casing, side plates, bearing supports, and lubricating interfaces form interacting sealing and frictional boundaries. Consequently, the outlet pressure is a dynamic signal containing shaft-order components, tooth-meshing harmonics, higher-order meshing multiples, and modulation sidebands [5][6][13][19]. These components are closely related to pump geometric periodicity and time-varying flow exchange between tooth spaces and inlet/outlet control volumes.

A physically interpretable description of pressure pulsation is essential for performance analysis and condition monitoring. Pressure pulsation affects hydraulic stability, noise generation, structural vibration, and downstream actuator performance [11][16]. Meanwhile, pressure signals contain fault-sensitive information related to internal leakage, side-plate wear, gear eccentricity, tooth-space filling, and local tooth damage [14][15][17][18]. Although data-driven methods have been widely applied to hydraulic-pump fault classification [17][18], they cannot independently explain why particular harmonics, meshing multiples, or modulation sidebands appear in the pressure spectrum. Mechanism-based modelling is therefore necessary when the objective is not only fault recognition but also physical interpretation.

Analytical and numerical studies have provided important foundations for understanding pressure and flow pulsation in external gear pumps. Early studies investigated cyclic excitation and theoretical flow ripple caused by the discrete displacement process [1][2]. Later work analysed pressure transients in meshing volumes, trapped-oil effects, tooth-space pressure evolution, incomplete filling, and cavitation-related flow variation using lumped-parameter modelling, control-volume methods, and CFD simulations [3][7][8][9][10][11][15]. Generalized control-volume models further showed that the pump fluid domain can be represented by interacting tooth-space regions, inlet and outlet control volumes, and trapped-oil volumes [7][8], linking geometric periodicity, leakage flow, and outlet pressure response.Although vibration analysis is widely used for gear-pump fault diagnosis, the present work focuses on the mechanism-level modelling of outlet pressure pulsation rather than on multisensor diagnostic classification.

A representative analytical framework is the rotational-frequency modulation model. In this framework, the pump chamber is divided into control volumes, and the pressure equation is established using the Eulerian description and continuity equation. Leakage through tooth-tip and tooth-side clearances is described using Couette--Poiseuille-type flow relations, while the outlet pressure is decomposed into low-frequency rotational components and high-frequency tooth-meshing components [7][8][12][19]. The resulting expression indicates that rotational-frequency components modulate the amplitude and phase of tooth-frequency and multiple tooth-frequency components, producing harmonic and sideband structures in the pressure spectrum [13][19].

However, most existing models focus on nominal pressure pulsation and do not explicitly introduce structural degradation variables. In practical external gear pumps, side-plate wear and gear tooth breakage are particularly important. Side-plate wear enlarges the effective side clearance and increases internal leakage; studies on volumetric efficiency, lateral lubricating interfaces, and wear degradation have confirmed that clearance variation directly affects leakage flow, pressure distribution, and pump performance [4][12][14]. Gear tooth breakage introduces a local periodic disturbance to the flow field and leads to pressure perturbations synchronized with gear rotation and meshing [5][6][17][20]. Thus, side-plate wear mainly changes the leakage-path geometry, whereas tooth breakage can alter both amplitude and phase characteristics of the pressure signal.

Recent interpretable diagnostic studies have introduced physical priors into hydraulic gear-pump fault modelling. Guan et al. proposed physically meaningful parameters related to side clearance and gear disturbance for compound fault diagnosis [20]. Inspired by this idea, the present work introduces the side-clearance parameter (d_{gap}) to represent leakage-path enlargement induced by side-plate wear, and uses (K_m) as an equivalent gear tooth-breakage disturbance intensity. The aim is not to construct a new tooth-contact or structural-impact model, but to incorporate tooth-breakage disturbance into the existing pressure-pulsation modulation framework.

Recent studies published in JDMD have also emphasised that compound-fault diagnosis should link fault-sensitive features to their underlying physical mechanisms,[21] while coupled gear-dynamic modelling can reveal harmonic responses associated with local defects.[22]

This paper develops a compound modulation model for outlet pressure pulsation in external gear pumps while preserving the flow-pressure-spectrum chain. Side-clearance is introduced at the leakage-flow level to describe amplitude-envelope variation, whereas tooth breakage is modelled as an equivalent periodic pressure disturbance and phase/frequency modulation source. The resulting Fourier-series expression incorporates both degradation sources, yielding a physically interpretable mechanism model.

2 Related Work and Physical Basis

2.1. Rotational-frequency-modulated pressure pulsation

Pressure pulsation in an external gear pump is fundamentally governed by the periodic motion of the gear pair and the resulting variation of internal control volumes. During gear rotation, tooth spaces are intermittently connected to the inlet and outlet chambers, while trapped-oil regions appear during double-tooth engagement. As a consequence, the outlet pressure is composed of low-frequency rotational components, tooth-meshing components, higher-order meshing harmonics, and modulation sidebands.

A representative mechanism-based description of this phenomenon is the rotational-frequency modulation model for gear-pump outlet pressure pulsation. In this framework, the pump fluid domain is divided into several control volumes, and the pressure variation in each control volume is derived from the continuity equation. In angular coordinates, the pressure evolution can be written as

$$\frac{dp}{d\theta} = \frac{B_{oil}}{V\omega}\left(\Delta Q - \omega\frac{dV}{d\theta}\right), \quad (1)$$

where B_{oil} is the bulk modulus of the hydraulic oil, V is the instantaneous control volume, ω is the gear angular velocity, and ΔQ is the net flow rate. This equation indicates that pressure pulsation is generated by the imbalance between flow exchange and control-volume variation.

The leakage through tooth-tip and tooth-side clearances is commonly represented by Couette-Poiseuille flow. For the i -th tooth-space control volume, the nominal leakage terms can be expressed as

$$Q_{h,i} = \frac{b_n h_i^3}{12\mu l_w}(p_i - p_{i-1}) + \frac{b_n\omega_n r_a h_i}{2},$$
$$Q_{f,i} = \frac{b_f h_f^3}{12\mu l_f}(p_i - p_{i-1}) + \frac{b_f\omega_n r_m h_f}{2}. \quad (2)$$

The first term in each expression is the pressure-driven Poiseuille component, which is cubic with respect to the clearance height, while the second term is the shear-driven Couette component caused by gear motion. Based on these flow terms, the outlet pressure can be decomposed into a low-frequency rotational component and a high-frequency tooth-meshing component. The essential conclusion of the rotational-frequency modulation model is that rotational-frequency components modulate both the amplitude and phase of tooth-frequency and tooth-frequency-multiple components.

Therefore, the original model provides the physical basis of the present work. Instead of replacing the established pressure-pulsation mechanism, this paper extends the same flow--pressure--spectrum chain by introducing two degradation-related modulation sources: side-clearance leakage and gear tooth-breakage disturbance.

2.2. Degradation-related modulation sources and modelling objective

In practical external gear pumps, side-plate wear and gear tooth breakage are two important structural degradation modes. Side-plate wear enlarges the effective sealing clearance between the gear end face and the side plate, thereby increasing the leakage path between high- and low-pressure regions. Its dominant physical influence is therefore associated with leakage-flow variation and pressure-pulsation amplitude modulation. Gear tooth breakage, by contrast, represents a local fracture or severe local material removal from a gear tooth. Since the damaged tooth repeatedly enters the meshing and flow-exchange regions, its pressure-side manifestation can be treated as an equivalent periodic hydraulic disturbance.

Following this physical interpretation, the side-clearance leakage and tooth-breakage disturbance can be compactly represented as

$$Q_{leak,d} = \frac{w d_{gap}^3}{12\mu L}\Delta P, Q_{br} = \frac{b_f\omega_n K_m d_{gap}}{2}, (3)$$

where d_{gap} denotes the equivalent side-clearance parameter, K_m denotes the equivalent gear tooth-breakage disturbance intensity, w and L are the equivalent width and length of the side leakage path, and ΔP is the pressure difference across the leakage channel. The first term shows that side-clearance enlargement enters the model through the cubic clearance dependence of leakage flow. The second term represents the equivalent hydraulic disturbance induced by gear tooth breakage and coupled with the clearance.

The tooth-breakage disturbance also introduces an additional frequency-domain effect. Based on the mapping between the gear disturbance parameter and the dominant pressure-pulsation frequency, the corresponding frequency and phase contribution can be written as

$$f_{puls} = \frac{\omega_n}{2\pi} + \sqrt{K_m},$$

$$\Phi_{K_m,m}(t) = 2\pi m\sqrt{K_m}t. \quad (4)$$

This term should be interpreted as an equivalent pressure-spectrum phase deviation caused by gear tooth breakage, rather than as a new structural impact or gear-mesh stiffness model.

Accordingly, side-clearance enlargement and gear tooth breakage play different roles in the outlet pressure spectrum. The former mainly modifies the amplitude envelope of tooth-frequency harmonics through leakage-path enlargement, whereas the latter contributes both an additional periodic pressure disturbance and an order-dependent phase/frequency deviation. The objective of this paper is therefore to establish an analytical outlet pressure pulsation model that simultaneously accounts for these two effects while retaining the original rotational-frequency modulation framework. The proposed model should be viewed as a mechanism-level extension of the existing pressure-pulsation formulation, rather than as a new gear-pump theory or a data-driven diagnostic classifier.

3 Methodology

This section develops the compound pressure-pulsation model by extending the physical basis introduced in Section 2. Since the control-volume pressure equation, the nominal Couette-Poiseuille leakage terms, and the degradation-induced flow sources have already been established, the following derivation focuses only on the necessary model extension: the modified tooth-side flow, the coupled outlet pressure equation, and the final Fourier representation of the outlet pressure pulsation.

3.1. Overall modelling framework

The proposed model follows the same flow--pressure--spectrum chain as the rotational-frequency modulation framework. First, the side-clearance parameter d_{gap} and the gear tooth-breakage disturbance intensity $K_m$are introduced into the tooth-side leakage-related flow term. Second, the modified flow term is substituted into the outlet control-volume pressure equation. Third, the resulting outlet pressure response is represented in a Fourier-series form, where side-clearance enlargement appears as an amplitude-envelope gain and tooth breakage appears as both an additional periodic pressure component and an order-dependent phase contribution.

This organization avoids directly imposing fault parameters on the final spectral coefficients. Instead, both degradation sources first enter the hydraulic flow balance and are then propagated to the pressure spectrum through the original outlet control-volume dynamics.

3.2. Modified tooth-side flow under coupled degradation

According to the physical basis discussed in Section 2, side-clearance enlargement primarily affects the pressure-driven leakage through its cubic clearance dependence, while gear tooth breakage introduces an additional hydraulic disturbance coupled with the clearance. Therefore, the nominal tooth-side flow can be extended as

$$Q_f^{dK} = \frac{b_f d_{gap}^3}{12\mu l_f}\Delta p + \frac{b_f \omega_n r_m d_{gap}}{2} + \frac{b_f \omega_n K_m d_{gap}}{2}, \tag{5}$$

where Δp denotes the pressure difference across the corresponding tooth-side leakage path. The first term represents the side-clearance-dependent Poiseuille leakage, the second term retains the shear-driven Couette contribution under the equivalent clearance, and the third term represents the gear tooth-breakage-induced hydraulic disturbance.

It should be emphasized that Eq.5 is not a new leakage theory. It is a compact reformulation of the nominal tooth-side leakage term after introducing the two degradation-related modulation sources. The side-clearance effect is therefore associated with leakage-amplitude variation, whereas the tooth-breakage effect is associated with an additional periodic disturbance superimposed on the flow exchange process.

3.3. Outlet pressure dynamics with side-clearance and tooth-breakage effects

For the outlet control volume, the tooth-side terms most directly affected by the coupled degradation are the leakage from the last driving and driven tooth spaces and the exchange between the trapped-oil region and the outlet. Replacing the corresponding nominal terms by their coupled-degradation forms gives

$$\frac{dp_{outH}^{dK}}{d\theta} = \frac{B_{oil}}{V_{out}\omega_n}\left(-Q_{T,out,atm} - Q_{h1,m} - Q_{h2,k} - 2Q_{f1,m}^{dK} - 2Q_{f2,k}^{dK} + 2Q_{f,t,out}^{dK} + 2Q_{T,t,out} - \omega_n\frac{dV_{out}}{d\theta}\right) \tag{6}$$

Equation (6). provides the direct bridge from the degradation-modified flow terms to the outlet pressure response. The model remains within the original control-volume framework, and no additional structural-impact, gear-mesh stiffness, bearing-dynamics, or CFD-based assumption is introduced.

The side-clearance contribution in the final spectral expression is represented by an equivalent amplitude gain. This gain is the Fourier-domain mapping of the pressure response induced by the cubic clearance-related leakage term, and can be written as

$$g_d(d_{gap})A_{mH} \equiv \mathcal{F}_m\left\{\mathcal{P}_{out}\left[\frac{b_f d_{gap}^3}{12\mu l_f}\Delta p\right]\right\}, \tag{7}$$

where $\mathcal{P}_{out}[\cdot]$ denotes the pressure response generated through the outlet control-volume dynamics, and $\mathscr{F}_m\{\cdot\}$denotes the extraction of the m-th tooth-frequency harmonic amplitude. Thus, $g_d(d_{gap})$ is not an arbitrary empirical coefficient, but a compact representation of the leakage-to-pressure-to-spectrum mapping.

Similarly, the equivalent pressure component caused by gear tooth breakage is defined as

$$p_{K_m}(t) \equiv \mathcal{P}_{out}\left[\frac{b_f \omega_n K_m d_{gap}(t)}{2}\right]. \quad (8)$$

This term should be understood as the pressure manifestation of the tooth-breakage-induced hydraulic disturbance after propagation through the outlet control volume. It is not an externally imposed impact waveform. The transfer coefficient k_{km} introduced below characterizes the contribution of this equivalent pressure disturbance to the amplitude modulation of tooth-frequency harmonics and should be identified from pressure measurements or a calibrated model.

3.4. Compound Fourier representation of outlet pressure pulsation

Following the original rotational-frequency modulation model, the outlet pressure is decomposed into a low-frequency rotational component and a high-frequency tooth-meshing component. The low-frequency component is retained as

$$p_{outL}(t) = A_{oL} + \sum_{n=1}^{6} A_{nL}\cos(n\omega_{oL}t + \psi_n), \quad (9)$$

Where A_{oL} is the constant component, A_{nL} and ψ_n are the amplitude and phase of the n-th rotational harmonic, and ω_{oL} is the rotational angular frequency observed at the outlet measuring point.

The amplitude-modulating and frequency-modulating parts of the low-frequency pressure are denoted as

$$p'_{oulL}(t) = A'\cos(\omega_{oL}t), \quad p''_{oulL}(t) = A''\sin(\omega_{oL}t). \quad (10)$$

These two quantities are retained from the original modulation model and describe the influence of rotational-frequency fluctuation on the amplitude and phase of the tooth-frequency pressure component.

Under nominal conditions, the high-frequency pressure pulsation component can be written as

$$p_{outH}(t) = A_{oH} + \sum_{m=1}^{6}[A_{mH} + k_{am}p'_{outL}(t)] \times \cos\left(m\omega_{oH}t + k_{fm}\int_0^t p'_{outL}(\tau)d\tau + \zeta_m\right). \quad (11)$$

whereA_{oH} is the high-frequency constant term,A_{mH} is the amplitude of the m -th tooth-frequency harmonic, ω_{oH} is the tooth-meshing angular frequency, k_{am} and k_{fm} are the amplitude- and frequency-modulation coefficients, and ζ_m is the initial phase.

By incorporating the side-clearance amplitude gain, the tooth-breakage pressure disturbance, and the tooth-breakage-induced phase contribution defined in Section2 , the compound outlet pressure pulsation is expressed as

$$p_{out}(t) = A_{oL} + \sum_{n=1}^{6} A_{nL}\cos(n\omega_{oL}t + \psi_n) + A_{oH} + \sum_{m=1}^{6}[g_d(d_{gap})A_{mH} + k_{am}p'_{outL}(t) + k_{km}P_{Km}(t)] \times \cos(m\omega_{oH}t + 2\pi m\sqrt{K_m}t + k_{fm}\int_0^t p''_{outL}(\tau)d\tau + \zeta_m) \quad (12)$$

Equation (12) is the core result of this paper. The first line describes the low-frequency rotational pressure component and the high-frequency constant component. The term $g_d(d_{gap})A_{mH}$ represents the side-clearance-induced correction to the tooth-frequency harmonic amplitude. The term $k_{am}p'_{outL}(t)$ retains the original rotational-frequency amplitude modulation. The term $k_{km}p_{K_m}(t)$represents the additional amplitude modulation caused by gear tooth breakage. In the phase function, $m\omega_{oH}t$ is the nominal tooth-frequency carrier phase,$2\pi m\sqrt{K_m}t$ is the gear tooth-breakage-induced phase contribution, and the integral term is the original rotational-frequency frequency modulation.

4 Experiments and Analysis

4.1.Experimental Setup and Fault Components

To verify the spectral characteristics of the proposed compound pressure pulsation model, experiments were conducted on an external gear pump test rig. The experimental platform consists of an external gear pump, a driving motor, a hydraulic loading circuit, pressure sensors, and a data acquisition system. The outlet pressure signal was

10.37965/jdmd.2026.1586

collected for pressure pulsation and spectral analysis.The pressure sensor was mounted immediately downstream of the pump discharge port, and its position was kept unchanged throughout all experiments.The installation position can affect the measured pulsation amplitude and phase because pipeline compliance, pressure-wave propagation, and local hydraulic resonance may attenuate or amplify particular frequency components. Therefore, the conclusions of this study are based on the relative spectral variations measured at this fixed location rather than on sensor-position-independent absolute amplitudes.

Figures belows show the experimental platform and the representative gear fault components. Figure 1. presents the external gear pump test rig and the pressure measurement arrangement. Figure 2. presents the corresponding gear fault components, including the normal gear, the end-face wear condition, and the tooth-breakage condition.Although vibration signals are widely used for general gear-pump fault diagnosis, the present study does not aim to perform multisensor fault classification. The governing equations directly describe outlet-pressure evolution, pressure harmonics, modulation sidebands, and reconstructed pressure components. Therefore, outlet pressure provides the most direct and internally consistent quantity for validating the proposed pressure-pulsation model. Pressure-only validation is sufficient for examining these pressure-domain relationships, but it should not be interpreted as showing that pressure is universally superior to vibration for all diagnostic tasks.

The experiments reported in this study were conducted using a CBW-10 external gear pump at a rotational speed of 1050 r/min. The outlet pressure was sampled at 20.48 kHz for at least 30 s in each run, and three repeated runs were performed for each fault condition. The outlet load or mean pressure was maintained at 0.5MPa, the working medium was XX oil, and the measured oil-temperature range was 25–30 ° C. The pressure sensor, with a measuring range of 0-1.6 MPa and an accuracy of 0.5% full scale, provided a 4–20 mA output to the data-acquisition system.

4.2.Spectral analysis under Different Fault Conditions

Figure 3.shows the outlet pressure spectra under healthy, gear end-face wear, and tooth-breakage conditions. The spectra are used to verify whether the proposed compound pressure pulsation model can provide a physically interpretable description of different degradation mechanisms. In the figure, the rotational-frequency components, tooth-frequency harmonics, and the local spectral components around the meshing-related frequencies are of particular interest.

Under the healthy condition, the outlet pressure spectrum is mainly dominated by the rotational-frequency components and the tooth-frequency harmonics. These components are caused by the periodic volume variation and gear meshing process of the external gear pump. Compared with the fault conditions, the healthy spectrum exhibits a relatively regular harmonic distribution, and no obvious additional modulation component appears around the tooth-frequency harmonics. This observation is consistent with the nominal part of the proposed pressure pulsation model.

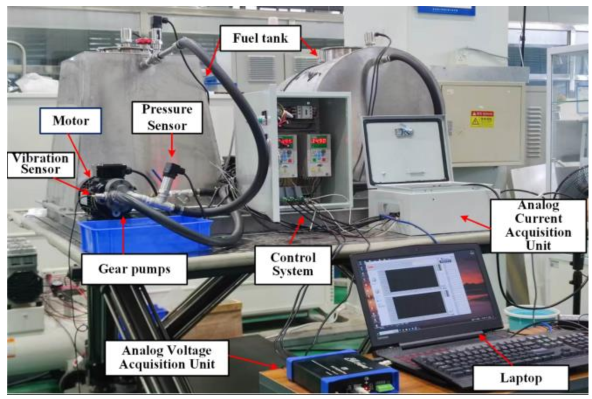

Fig. 1. Experimental test rig and pressure-sensor arrangement.

Fig. 2. Representative gear fault components

For the gear end-face wear condition, the amplitudes of the tooth-frequency harmonics and their multiples show noticeable variation. This phenomenon is physically reasonable because end-face wear increases the equivalent end-face clearance and strengthens the internal leakage path in the outlet control volume. Therefore, gear end-face wear can be interpreted as an equivalent clearance-related leakage degradation. In the proposed model, this effect is represented by the leakage-induced amplitude correction term $g_d(d_{gap})A_{mH}$. The corresponding spectral influence is mainly reflected in the amplitude-envelope variation of tooth-frequency harmonics rather than the generation of a completely new independent carrier frequency.

For the tooth-breakage condition, the spectrum exhibits a more complex distribution of local spectral components, especially in the low-frequency and dominant harmonic-related regions. Compared with the healthy and gear end-face wear conditions, the tooth-breakage spectrum contains denser spectral components and more evident local amplitude fluctuation around several dominant peaks. This phenomenon indicates that tooth breakage may introduce additional periodic pressure disturbance and modulation effects during the meshing process.This is because tooth breakage destroys the uniform meshing process and introduces a local periodic pressure disturbance when the damaged tooth passes through the meshing region. In the proposed model, this effect is described by the additional pressure disturbance term $k_{km}p_{K_m}(t)$ and the order-dependent phase deviation term $2\pi m\sqrt{K_m}t$. Therefore, the tooth-breakage spectrum reflects not only harmonic-amplitude variation but also modulation-related spectral changes around the meshing harmonics.

The comparison among the three conditions indicates that gear end-face wear and tooth breakage affect the outlet pressure spectrum through different physical paths. Gear end-face wear mainly changes the leakage balance and modifies the amplitude envelope of the tooth-frequency components, whereas tooth breakage introduces additional periodic disturbance and phase modulation, leading to sideband growth and local spectral deformation. These observations support the spectral interpretation of the proposed compound pressure pulsation model.

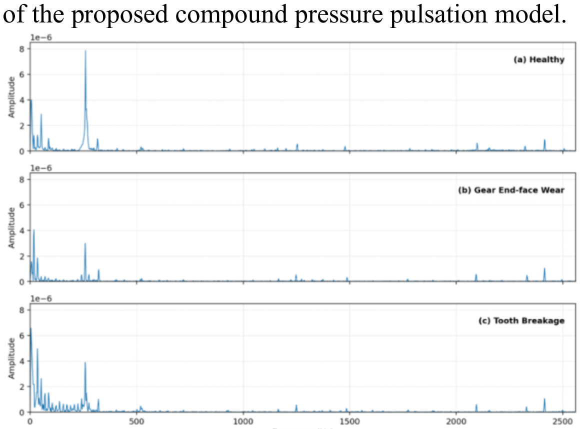

Fig.3.pressure spectra under different fault conditions.

4.3.Time-DomainPressure Reconstruction and Model Validation

To further validate the effectiveness of the proposed compound pressure pulsation model, time-domain pressure reconstruction is performed for the gear end-face wear and tooth-breakage conditions. These two fault states are selected because they correspond to the two main degradation paths considered in the proposed model, namely leakage-induced amplitude correction and tooth-breakage-induced modulation disturbance. The purpose of this validation is to examine whether the proposed model can reproduce the dominant periodic pressure fluctuation of the measured outlet pressure under typical degradation conditions. Based on the compound Fourier representation in Eq.(12), the model parameters are identified from the measured outlet pressure signal and then substituted into the reconstructed pressure expression. The reconstructed pressure signal can be written as

$$p_{out}^{rec}(t) = p_{outL}^{rec}(t) + p_{outH}^{rec}(t), \qquad (13)$$

where $p_{outL}^{rec}(t)$ denotes the reconstructed low-frequency rotational component, and$p_{outH}^{rec}(t)$denotes the reconstructed high-frequency tooth-meshing component with degradation-related modulation. For the gear end-face wear condition, the reconstruction mainly depends on the leakage-induced amplitude correction term $g_d(d_{gap})A_{mH}$, which modifies the amplitude envelope of the tooth-frequency harmonic components. For the tooth-breakage condition, the additional pressure disturbance term $k_{km}p_{K_m}(t)$ and the order-dependent phase deviation term $2\pi m\sqrt{K_m}t$ are introduced to describe the modulation effect caused by local tooth damage. The time-domain reconstruction error is evaluated by the difference between the measured and reconstructed outlet pressure signals:

$$J_t = \|p_{out}^{meas}(t) - p_{out}^{rec}(t)\|_2^2, \qquad (14)$$

where $p_{out}^{meas}(t)$ denotes the measured outlet pressure signal, and $p_{out}^{rec}(t)$ denotes the model-reconstructed pressure signal. This objective is used to evaluate the waveform-level consistency between the measured and reconstructed pressure pulsations. In practical implementation, the identified parameters are treated as equivalent pressure-spectrum parameters, so that the reconstruction focuses on the dominant rotational, tooth-meshing, and modulation-related components rather than all broadband noise components.The reconstruction is intended to recover the deterministic rotational, tooth-meshing, and modulation-related components retained by Eq. (12), rather than random broadband noise or transient measurement disturbances. Consequently, local pointwise differences between the measured and reconstructed signals are expected. Agreement in the dominant periodic components and their amplitude envelopes is therefore taken as the relevant validation criterion.

Figure.4 shows the comparison between the measured and reconstructed outlet pressure signals under gear end-face wear and tooth-breakage conditions. For the gear end-face wear condition, the reconstructed signal follows the main periodic fluctuation of the measured pressure signal. This indicates that the leakage-induced amplitude correction term can effectively describe the amplitude-envelope variation caused by end-face wear. The agreement between the measured and reconstructed waveforms demonstrates that the equivalent clearance-related leakage effect is reflected not only in the frequency spectrum, but also in the time-domain pressure response.

For the tooth-breakage condition, the reconstructed signal also captures the dominant periodic fluctuation of the measured pressure signal. Compared with the gear end-face wear condition, tooth breakage introduces more complex local waveform variation because the damaged tooth repeatedly enters the meshing and flow-exchange regions. The good agreement between the measured and reconstructed signals indicates that the additional pressure disturbance and phase-deviation terms can describe the tooth-breakage-induced modulation effect in the outlet pressure response. The reconstruction results demonstrate that the proposed compound pressure pulsation model is not limited to qualitative spectral interpretation. By combining the nominal rotational-frequency modulation, the leakage-related amplitude correction, and the tooth-breakage-induced pressure and phase modulation, the model can reproduce the dominant time-domain pressure pulsation under representative degradation conditions. Therefore, the measured--reconstructed waveform comparison provides direct evidence for the physical validity of the proposed model.

5 Conclusion and Future Work

This paper developed a compound pressure pulsation model for external gear pumps by incorporating side-clearance leakage and gear tooth-breakage modulation into the conventional rotational-frequency modulation framework. The proposed model preserves the original flow--pressure--spectrum chain and introduces two physically interpretable degradation parameters. The side-clearance-related term describes the leakage-induced amplitude correction of tooth-frequency harmonics, while the tooth-breakage-related term represents both an additional periodic pressure disturbance and an order-dependent phase deviation. Therefore, the model provides a mechanism-level explanation for amplitude-envelope variation, sideband enhancement, local spectral broadening, and possible shifted meshing-related components in the outlet pressure spectrum.

Experimental spectral analysis under healthy, gear end-face wear, and tooth-breakage conditions further supports the proposed interpretation. Gear end-face wear mainly changes the leakage balance and modifies the amplitudes of tooth-frequency harmonics, whereas tooth breakage introduces stronger local modulation around meshing harmonics. The comparison between measured and reconstructed outlet pressure also shows that the proposed formulation can describe the dominant pressure pulsation behavior in both time and frequency domains. These results indicate that the model can serve as a physically interpretable basis for pressure-spectrum analysis of external gear pumps under coupled degradation conditions.The present validation is limited to a single controlled rotational speed of 1050 r/min and a small number of representative fault states and fault severities. The effects of load variation, oil temperature, manufacturing variability, and pressure-sensor position have not yet been systematically quantified. Therefore, the identified parameters should not be interpreted as universally transferable diagnostic thresholds.

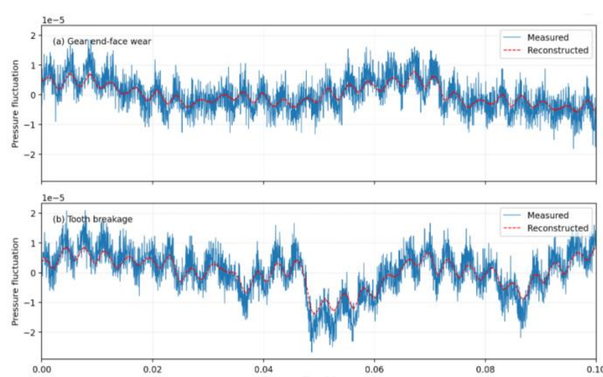

Fig.4. Time-domain comparison between measured and reconstructed outlet pressure signals.

Future work will focus on three aspects. First, more controlled experiments will be conducted under different speeds, loads, and degradation severities to quantitatively identify the model parameters. Second, independent clearance, leakage, and fault-severity measurements will be introduced to further calibrate the mapping between physical degradation and spectral parameters. Third, the proposed mechanism model will be combined with data-driven diagnostic methods to improve fault interpretation and robustness under complex operating conditions.In future diagnostic applications, the identified clearance-related amplitude gain and tooth-breakage disturbance and phase terms may be converted into physically interpretable health indicators. Their variations, together with meshing-harmonic amplitudes and sideband energy, could support fault-type discrimination and degradation-severity tracking. These quantities may also be introduced as physics-informed features or constraints in data-driven diagnostic models.

To further validate the effectiveness of the proposed compound pressure pulsation model, the identified model parameters are substituted into the reconstructed outlet pressure expression and compared with the measured pressure signal. The comparison is conducted in both the time domain and the frequency domain, so that the waveform-level consistency and the spectral reconstruction capability can be evaluated simultaneously.

Figure 4.shows the comparison between the measured outlet pressure and the model-reconstructed pressure. In the time domain, the reconstructed signal follows the main periodic fluctuation of the measured pressure, indicating that the proposed model can describe the dominant pressure pulsation behavior of the external gear pump. In the frequency domain, the reconstructed spectrum preserves the main rotational-frequency components, tooth-frequency harmonics, and meshing-related spectral structures observed in the measured spectrum.

For the gear end-face wear condition, the reconstruction improvement mainly comes from the leakage-induced amplitude correction term $g_d(d_{gap})A_{mH}$, which adjusts the amplitude envelope of the tooth-frequency harmonics. For the tooth-breakage condition, the additional disturbance term $k_{km}p_{K_m}(t)$ and the order-dependent phase deviation term $2\pi m\sqrt{K_m}t$ help describe the local modulation characteristics around the meshing harmonics, including sideband enhancement and local spectral broadening.

The reconstruction result demonstrates that the proposed compound model is not limited to qualitative spectral interpretation. It can also provide a quantitative reconstruction of the outlet pressure response by combining the nominal rotational-frequency modulation, the leakage-related amplitude correction, and the tooth-breakage-induced pressure and phase modulation. Therefore, the measured--reconstructed comparison provides direct evidence for the physical validity of the proposed model.

6 References

[1] K. Foster, R. Taylor, I. M. Bidhendi, "Computer prediction of cyclic excitation sources for an external gear pump," Proceedings of the Institution of Mechanical Engineers, Part B, Vol. 199, No. 3 (1985).

[2] N. D. Manring, S. B. Kasaragadda, "The theoretical flow ripple of an external gear pump," Journal of Dynamic Systems, Measurement and Control, Vol. 125, No. 3 (2003).

[3] M. Borghi, M. Milani, F. Paltrinieri, B. Zardin, "Pressure transients in external gear pumps and motors meshing volumes," SAE Technical Paper, No. 2005-01-3619 (2005).

[4] M. Borghi, B. Zardin, E. Specchia, "External gear pump volumetric efficiency: Numerical and experimental analysis," SAE Technical Paper, No. 2009-01-2844 (2009).

[5] E. Mucchi, G. Dalpiaz, A. Fernάndez del Rincó n, "Elastodynamic analysis of a gear pump. Part I: Pressure distribution and gear eccentricity," Mechanical Systems and Signal Processing, Vol. 24, No. 7 (2010).

[6] E. Mucchi, G. Dalpiaz, A. Rivola, "Elastodynamic analysis of a gear pump. Part II: Meshing phenomena and simulation results," Mechanical Systems and Signal Processing, Vol. 24, No. 7 (2010).

[7] S. Wang, H. Sakura, A. Kasarekar, "Numerical modelling and analysis of external gear pumps by applying generalized control volumes," Mathematical and Computer Modelling of Dynamical Systems, Vol. 17, No. 5 (2011).

[8] A. Vacca, M. Guidetti, "Modelling and experimental validation of external spur gear machines for fluid power applications," Simulation Modelling Practice and Theory, Vol. 19, No. 9 (2011).

[9] J. Zhou, A. Vacca, P. Casoli, "A novel approach for predicting the operation of external gear pumps under cavitating conditions," Simulation Modelling Practice and Theory, Vol. 45 (2014).

[10] X. Hao, X. Zhou, X. Liu, X. Sang, "Flow characteristics of external gear pumps considering trapped volume," Advances in Mechanical Engineering, Vol. 8, No. 10 (2016).

[11] E. Frosina, A. Senatore, M. Rigosi, "Study of a high-pressure external gear pump with a computational fluid dynamic modeling approach," Energies, Vol. 10, No. 8 (2017).

[12] D. Thiagarajan, A. Vacca, "Mixed lubrication effects in the lateral lubricating interfaces of external gear machines: Modelling and experimental validation," Energies, Vol. 10, No. 1 (2017).

[13] X. Zhao, A. Vacca, "Theoretical investigation into the ripple source of external gear pumps," Energies, Vol. 12, No. 3 (2019).

[14] R. Guo, Y. Li, Y. Shi, H. Li, J. Zhao, D. Gao, "Research on identification method of wear degradation of external gear pump based on flow field analysis," Sensors, Vol. 20, No. 14 (2020).

[15] A. Corvaglia, M. Rundo, P. Casoli, A. Lettini, "Evaluation of tooth space pressure and incomplete filling in external gear pumps by means of three-dimensional CFD simulations," Energies, Vol. 14, No. 2 (2021).

[16] S. Woo, A. Vacca, "An investigation of the vibration modes of an external gear pump through experiments and numerical modeling," Energies, Vol. 15, No. 3 (2022).

[17] Z. Liu, Y. Liu, H. Shan, B. Cai, Q. Huang, "A fault diagnosis methodology for gear pump based on EEMD and Bayesian network," PLOS ONE, Vol. 10, No. 5 (2015).

[18] Y. Yang et al., "Current status and applications for hydraulic pump fault diagnosis: A review," Sensors, Vol. 22, No. 24 (2022).

[19] W. Xu, Z. Wang, Z. Zhou, C. Sun, J. Zhang, R. Yan, X. Chen, "An advanced pressure pulsation model for external gear pump," Mechanical Systems and Signal Processing, Vol. 187 (2023).

[20] T. Guan, D. Gao, J. Ma, J. Wu, S. Wang, C. Zhang, L. Wang, J. Tang, "Interpretable compound fault diagnosis of hydraulic gear pumps via fusion of physical priors and probabilistic joint reasoning," Mechanical Systems and Signal Processing, Vol. 243 (2026).

[21] R. Huang, J. Xia, B. Zhang, Z. Chen, and W. Li, “Compound Fault Diagnosis for Rotating Machinery: State-of-the-Art, Challenges, and Opportunities,” Journal of Dynamics, Monitoring and Diagnostics, vol. 2, no. 1, pp. 13–29, 2023, doi: 10.37965/jdmd.2023.152.

[22] Y. Han, X. Chen, J. Xiao, J. X. Gu, and M. Xu, “An Improved Coupled Dynamic Modeling for Exploring Gearbox Vibrations Considering Local Defects,” Journal of Dynamics, Monitoring and Diagnostics, vol. 2, no. 4, pp. 262–274, 2023, doi: 10.37965/jdmd.2023.186.